Monthly Notices
of the
ROYAL ASTRONOMICAL SOCIETY
MNRAS **445,** 2223–2231 (2014) doi:10.1093/mnras/stu1812

On the mass estimation for FGK stars: comparison of several methods

F. J. G. Pinheiro,[1,2]★ J. M. Fernandes,[1,2,3] M. S. Cunha,[4,5] M. J. P. F. G. Monteiro,[4,5,6] N. C. Santos,[4,5,6] S. G. Sousa,[4,5,6] J. P. Marques,[7] J.-J. Fang,[8] A. Mortier[9] and J. Sousa[4,5]

[1]*Centro de Geofísica da Universidade de Coimbra, P-3040-004 Coimbra, Portugal*
[2]*Observatório Geofísico e Astronómico da Universidade de Coimbra, P-3040-004 Coimbra, Portugal*
[3]*Departamento de Matemática da Universidade de Coimbra, Largo D. Dinis, P-3001-454 Coimbra, Portugal*
[4]*Instituto de Astrofísica e Ciências do Espaço, Universidade do Porto, CAUP, Rua das Estrelas, PT4150-762 Porto, Portugal*
[5]*Centro de Astrofísica, Universidade do Porto, Rua das Estrelas, P-4150-762 Porto, Portugal*
[6]*Departamento de Física e Astronomia, Faculdade de Ciências, Universidade do Porto, P-4150-762 Porto, Portugal*
[7]*The Institut d'Astrophysique Spatiale, F-121 91405 Orsay, France*
[8]*Centro de Física Computacional, Department of Physics, University of Coimbra, P-3004-516 Coimbra, Portugal*
[9]*SUPA, School of Physics and Astronomy, University of St Andrews, St Andrews KY16 9SS, UK*

Accepted 2014 September 3. Received 2014 September 3; in original form 2013 November 11

ABSTRACT

Stellar evolutionary models simulate well binary stars when individual stellar mass and system metallicity are known. The mass can be derived directly from observations only in the case of multiple stellar systems, mainly binaries. Yet, the number of such stars for which accurate stellar masses are available is rather small. The main goal of this project is to provide realistic mass estimates for a homogeneous sample of about a thousand FGK single stars, using four different methods and techniques. We present the masses inferred according to each one of these methods as well as a final mass estimate consisting in the median of the four mass estimates. The procedures evaluated here include the use of stellar evolutionary models, mass–luminosity relation and surface gravity spectroscopic observations. By combining the results obtained with different methods, we determine the best mass value for each individual star, as well as the associated error budget. Our results confirm the expected consistency between the different mass estimation methods. None the less, for masses above 1.2 $M_{\odot}$, the spectroscopic surface gravities seem to overestimate the mass. This result may be a consequence of the spectroscopic surface gravities used in this analysis. Nevertheless, this problem is minimized by the fact that we have several approaches available for deriving stellar masses. Moreover, we suggest an empirical procedure to overcome this issue.

Key words: methods: numerical – binaries: general – stars: fundamental parameters – Hertzsprung–Russell and colour–magnitude diagrams.

1 INTRODUCTION

The mass is a fundamental stellar parameter. Moreover, the stellar mass has a major impact in other astrophysical contexts, such as in studies of the initial mass function, of the mass–luminosity relation (MLR), the study of extra-solar planets and their frequency for stars of different masses, and of the definition of the star–brown dwarf limit. All these aspects are fundamental when studying the global proprieties of the Galaxy, and when attempting to improve the characterization of stellar populations in galaxies.

Stellar masses can be determined with accuracy only for visual, spectroscopic and eclipsing binaries. For the latter, an accuracy of 1–3 per cent can be achieved (Andersen 1991; recently revised by Torres, Andersen & Giménez 2010). Unfortunately, the number of stars for which accurate stellar masses are available is less than 180 (Torres et al. 2010). Moreover, in most cases these are members of eclipsing binaries for which the metallicity (for example) is currently unknown or poorly known. Different methods are commonly used to determine the mass of single stars. In particular, for FGK stars we can find semi-observational, empirical and theoretical methods for mass determination.

As a semi-observational method, we may consider the determination of the mass through the surface gravity. Spectroscopic analysis of a star allows for the determination of effective

★ E-mail: fpinheiro@teor.fis.uc.pt

temperature, metallicity and surface gravity (e.g. Santos et al. 2005; Sousa et al. 2006). Currently, the knowledge of the photometry (including bolometric correction) and parallax allows the luminosity (L) to be determined and then the mass can be estimated. This methodology is potentially interesting for nearby stars, where the uncertainty in the distance (and thus in the luminosity) is more likely to be small. Errors affecting this method include the usually high uncertainties in the spectroscopic surface gravities, or for the case of stars at more than 50 pc, the errors in the measured parallax (for some stars, this problem will be solved with the *Gaia* mission). The present accuracy on the mass determinations using this method is not better than 10–20 per cent (Sousa et al. 2011a).

As an empirical method we may consider the determination of mass through the MLR. Henry (2004) published the best known MLR for stars ranging in mass from 0.07 up to 33 $M_{\odot}$. If the luminosity is known, this relation allows an estimation of the stellar mass with an accuracy of 8–10 per cent (depending on the mass range, e.g., Henry & McCarthy 1993). More recently, Xia & Fu (2010) published an MLR using 203 main-sequence stars (with spectral types ranging from O to K), obtaining a relative error on the mass estimation of about 5 per cent. One of the major drawbacks of the MLR is the (quantitatively) unknown contribution of the evolution and chemical composition of different stars to the intrinsic dispersion (e.g. Gafeira, Patacas & Fernandes 2012).

Regarding a theoretical method, we consider the mass estimation through stellar models in the Hertzsprung–Russell (HR) diagram and/or using asteroseismology. The former is the most current method used to estimate the mass. Pre-computed (grids of) stellar evolutionary models are compared to luminosity and effective temperature on the HR diagram. This is frequently known as an HR diagram analysis. The degeneracy between mass and other parameters, like the abundance of helium and metals, results in a systematic uncertainty of this method (accuracy) of the order of 10 per cent (Fernandes & Santos 2004). On the other hand, several asteroseismic tools for the determination of stellar masses of solar-type stars have been developed for application to stars whose oscillation spectra have already been observed thanks, in particularly, to projects as *Kepler* or *CoRoT* (Metcalfe et al. 2010; Bigot et al. 2011). Asteroseismology complements the global observables available for a single star. This technique can result in mass uncertainties below 5 per cent if a few frequencies with an uncertainty below 0.1 μHz are available (e.g. Kjeldsen, Bedding & Christensen-Dalsgaard 2009; Huber et al. 2012; Mathur et al. 2012; Creevey et al. 2013; Chaplin et al. 2014 and references therein). The main drawback for this is the fact that the number of stars that fulfil the above precision in frequencies is still small.

We would like to stress that one of the strongest advantages of this work is the fact that we treat a large and homogeneous sample of 451+582 FGK stars from the works of Sousa et al. (2006, 2008, 2011b) and Santos et al. (2005). All the stars were spectroscopically analysed by the same technique and procedure. We recall that the study of the frequency of extra-solar planets as a function of stellar mass is a stronger constraint to the formation of exoplanets. Only a few studies have discussed this issue, and no major correlation has yet been found for solar-type stars, possibly due to the relatively large error bars in the determination of stellar masses (e.g. Johnson et al. 2010; Mortier et al. 2013a; Neves et al. 2013).

Our paper is organized as follows. The observational data are discussed in Section 2, where the different methods used to estimate the stellar mass are described. We then report and discuss in Section 3 the results for the selected sample. Finally, in Section 4, we draw some conclusions and suggest future work.

2 OBSERVATIONAL DATA AND METHODOLOGY

The objects used in our analysis were taken from the works of Sousa et al. (2008, 2011b) for which information on their effective temperature ($T_{\rm eff}$), luminosity (L), surface gravity ($\log g$) and metal abundance ([Fe/H]) has been derived in a consistent way. This sample comprises more than a thousand objects located in the solar neighbourhood (up to 58 pc away), presenting slow rotation velocities and no signs of stellar activity, for which any known binaries and variable stars have been excluded (Sousa et al. 2008, 2011b). A detailed description of these targets can be found in the works of Mayor et al. (2003) and Lo Curto et al. (2010). In general terms, the global properties of these targets are within the range of those typical for FGK-type stars ($3.68 < \log(T_{\rm eff}) < 3.86$; $-1.3 < \log(L/L_{\odot}) < 1.04$; $3.7 < \log(g) < 4.5$ and $-1.14 < [{\rm Fe}/X] < 0.07$). The luminosities were derived following the same procedure described by Santos, Israelian & Mayor (2004), which is based on the parallaxes from *Hipparcos* (van Leeuwen 2007), the respective magnitudes and the bolometric corrections from Flower (1996). The spectroscopic surface gravity inferences of Sousa et al. used in our study are determined with the ARES+MOOG codes. These computations are based on equivalent widths of iron lines. Unlike other works, the computations based on specific line list of Sousa et al. (2008) show little dependence between surface gravities and effective temperature (Mortier et al. 2013b). A similar behaviour was also shown in the paper from Torres et al. (2012) for a similar procedure also based on equivalent widths. The reason for this is that the surface gravity is constrained using the Fe I lines that are much less in number than the Fe I lines that are used to constrain the effective temperature.

Taking into account these global properties, we apply four different mass inference approaches.

Method 1– 'Direct' determination of the stellar mass by taking into account surface gravities and stellar radii derived from the well-known luminosity–radius–effective temperature relation. In the particular case of using a spectroscopic surface gravity, one obtains what is known as the spectroscopic mass. Mortier et al. (2013b) discuss the impact that different methods of surface gravity estimation can have on the determination of stellar masses. In a similar way, Huber et al. (2012) compare asteroseismic surface gravities with those obtained from the analysis of photometric light curves.

Method 2– Use of the Torres et al. (2010) empirical relation between stellar mass, effective temperature, surface gravity and metal abundance, derived from the analysis of stellar binaries:

$$\log\left(\frac{M}{M_{\odot}}\right) = a_1 + a_2 X + a_3 X^2 + a_4 X^3 + a_5 (\log g)^2 + a_6 (\log g)^3 + a_7 [{\rm Fe/H}], \quad (1)$$

where $X = \log(T_{\rm eff}) - 4.1$, $a_1 = 1.5689\pm0.058$, $a_2 = 1.3787\pm0.029$, $a_3 = 0.4243\pm0.029$, $a_4 = 1.139\pm0.24$, $a_5 = -0.1425\pm0.011$, $a_6 = 0.019\,69\pm0.0019$, $a_7 = 0.1010\pm0.014$ and $M_{\odot}$ is the solar mass. For main-sequence stars with masses above 0.6 $M_{\odot}$, the scatter for this calibration is $\sigma_{\log M/M_{\odot}} = 0.027$. Notice that there is a slight offset between the solar mass and the one expected from this method. Santos et al. (2013) propose a calibration of these results similar to the predictions of the Padova isochrones.

Method 3– Use of the empirical MLR of Henry & McCarthy (1993), calibrated by taking into account binary stars, which for

stars ranging between 0.5 and 2.0 $M_\odot$ is

$$\log\left(\frac{M}{M_\odot}\right) = 2.456\times10^{-3}M_v^2 - 9.711\times10^{-2}M_v + 4.365\times10^{-1}, \quad (2)$$

in which absolute magnitudes (M_v) were derived taking into account the bolometric correction of Torres (2010). In this case, the root mean square (rms) of the fit is 0.032 (in $\log M/M_\odot$).

Method 4– Comparison of the targets' position in the HR diagram against the theoretical predictions of the Padova isochrones (as in Fernandes, Vaz & Vicente 2011). This is done through a χ^2 minimization procedure, by minimizing the following quantity:

$$S = \sum_{i=1,4}\left(\frac{X_i - X_{\rm model}}{\Delta X_i}\right)^2, \quad (3)$$

in which X_i is one of the four observables (L, $T_{\rm eff}$, $\log g$ and [Fe/H]) and ΔX_i is the uncertainty associated with it. Notice that in the case of the Sun, the models used here fail to predict its mass by 0.023 $M_\odot$. For this reason, we associate a 0.05 $M_\odot$ systematic uncertainty to this method .

The asteroseismic properties of solar-type stars can also be used to infer stellar masses. Indeed, there are two relationships relating the stellar density and surface gravity with the large frequency separation $\Delta\nu_0$, i.e. the separation between modes of the same degree and consecutive radial order (Ulrich 1986) and the frequency $\nu_{\rm max}$ at which solar-type oscillations have maximum power (Brown et al. 1991; Kjeldsen & Bedding 1995). Unfortunately, unlike in the case of the work of Bruntt et al. (2010), our data set contains no such asteroseismic information. Therefore, we cannot apply the latter approach.

For all methods, Monte Carlo simulations were used to infer the mass uncertainties that arise from the uncertainties on the global stellar parameters. Moreover, in the case of the empirical approaches and the HR diagram analysis, our Monte Carlo simulations also took into account the systematic uncertainties associated with these methods (in particular uncertainty associated with the goodness of the empirical fits).

Given these four mass estimates, we want to investigate the better way to use the four mass predictions available minimizing the impact of any outlier values in the final mass estimate. For this reason, we evaluated three different methods for merging this information into a single mass prediction: the computation of the statistical mean, the median and a weighted mean:

$$M = \left(\sum_{i=1}^{4} M_i w_i\right) \times \left(\sum_{i=1}^{4} w_i\right)^{-1}, \quad (4)$$

where $w_i = 1/\sigma_i^2$ and σ_i is the mass uncertainty associated with method 'i'.

3 RESULTS AND DISCUSSION

Fig. 1 shows a comparison between the mass estimates, obtained according to each method, for data from Sousa et al. As a reference, we also plotted each method's prediction for 22 stars from the work of Bruntt et al. (2010).

In the latter case, we took into account the luminosities, spectroscopic effective temperatures and metal abundances provided by Bruntt et al. On the other hand, surface gravities were derived using the expression of Kjeldsen & Bedding (1995), relating the stellar surface gravity with the frequency of maximum power oscillations (equation 5 in their work).

Fig. 1 and Table 1 point out towards relatively good agreement between both empirical methods and the predictions of the Padova isochrones. Indeed, a linear fit to these methods' predictions lies close to the expected 1:1 relation.

The scatter of the data can be partially explained by the uncertainties associated with each method's predictions. However, for higher masses ($M > 1.1\,M_\odot$), this no longer occurs between these three methods' predictions and some of the (direct) spectroscopic masses of Sousa et al.'s targets. This could be a source of concern since, in theory, the 'direct' approach could be seen as the most reliable approach. Unlike the other methods, it relies exclusively on well-known physical relationships between global stellar parameters (instead of empirical relationships or models). Nevertheless, an inspection of the masses inferred for Bruntt et al.'s targets clearly shows that the 1:1 relation between the four mass predictions is reasonably satisfied. This indicates that the problem must lie on the values of the global parameters used in these computations and not on the methods themselves.

A simple test to the Sousa et al. (2011b) data revealed that, from the four approaches considered here, the direct method is the most sensitive to errors in the luminosity and effective temperature. The test consisted in introducing a 0.05 dex increase on the surface gravity and luminosity of each star and determining the corresponding impact on the final mass estimate (see Fig. 2). This analysis only evaluates the individual impact that these parameters have on the mass determination. Correlations between the effective temperature and surface gravity uncertainties were disregarded since the computations based on the specific line list of Sousa et al. (2008) show little dependence on surface gravities and effective temperature (Mortier et al. 2013b). In this way, we observed that the fraction of stars in the sample which suffer a significant mass shift when this procedure is applied is largest for the spectroscopic approach. This provides a plausible justification for the weaker agreement between the spectroscopic masses and other mass estimates.

After finding a possible justification for the discrepancy between the different mass estimations, we proceeded to identify the stellar parameter causing this discrepancy. In order to do so, we require what can be called as the 'final mass estimate', which results from combining the four individual estimates. An inspection to Fig. 3 shows that, as it should be expected, the non-weighted average can be strongly affected by errors in a given mass estimate. On the other hand, the median and the weighted mean of the mass estimates are very close to the 1:1 relation. For instance, for the Sousa et al. (2008) data, we get $M_{\rm Weighted} = 0.92M_{\rm Median} + 0.04$. Moreover, an inspection of the rms between the different mass estimates (Table 2) shows that both, the weighted mass and the median of the four mass estimates, are equally good for combining the four values. The rms between the median and the weighted averages is 0.055 for the 2008 and 0.053 for the 2011 data. Again, this result points out the similarities between these methods of mass combination.

The main problem of using a non-weighted average is that errors in one of the mass estimates can have a significant impact on the final result (as it will be seen later in Table 2 and Fig. 3). Moreover, the error associated with a given mass estimate may not necessarily reflect the reliability of its corresponding mass estimation method. On the other hand, medians are good indicators of central tendencies which tend to be far less sensitive to such issues. Thus, given the median's robustness to outliers, it was decided to use this value as the 'final' mass estimate.

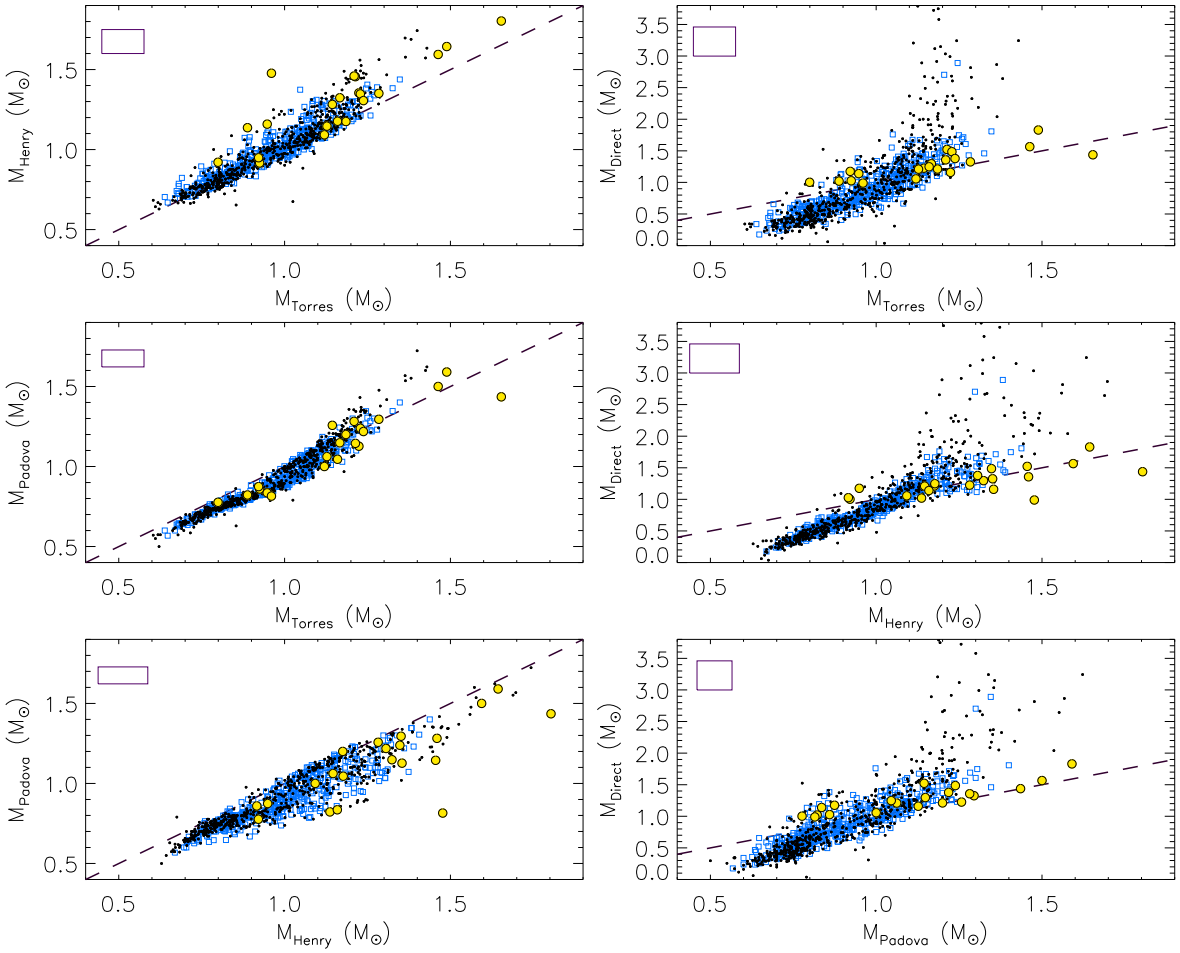

Figure 1. Comparison between the mass estimates obtained using the different methods. The squares and black dots correspond, respectively, to the Sousa et al. (2008, 2011b) data, while the circles correspond to the Bruntt et al. (2010) data. The boxes on the top left of each panel correspond to the typical mass uncertainties associated with each method, while the dashed line shows the 1:1 relation expected if each two methods were in perfect agreement.

Table 1. Comparison between different mass estimation methods for the Sousa et al. (2008, 2011a) and Bruntt et al. (2010) data, including the root mean square of the mass estimates and a linear fit with parameters (a, b) to these predictions, given by $M_2 = aM_1 + b$ (last column).

	M_1	M_2	$\mathrm{rms}_{M1\text{-}M2}$	(a, b)
	M_{Torres}	M_{Henry}	0.067	(1.02, +0.01)
	M_{Torres}	M_{Padova}	0.072	(1.07, −0.13)
Sousa et al. (2008)	M_{Henry}	M_{Padova}	0.115	(0.91, −0.00)
	M_{Torres}	M_{Direct}	0.260	(2.15, −1.19)
	M_{Henry}	M_{Direct}	0.247	(2.12, −1.24)
	M_{Padova}	M_{Direct}	0.233	(1.99, −0.92)
	M_{Torres}	M_{Henry}	0.089	(1.17, −0.13)
	M_{Torres}	M_{Padova}	0.073	(1.17, −0.21)
Sousa et al. (2011b)	M_{Henry}	M_{Padova}	0.110	(0.91, +0.01)
	M_{Torres}	M_{Direct}	0.544	(3.24, −2.12)
	M_{Henry}	M_{Direct}	0.494	(2.81, −1.82)
	M_{Padova}	M_{Direct}	0.506	(2.89, −1.67)
	M_{Torres}	M_{Henry}	0.183	(1.05, +0.07)
	M_{Torres}	M_{Padova}	0.177	(1.42, −0.51)
Bruntt et al. (2010)	M_{Henry}	M_{Padova}	0.241	(1.18, −0.38)
	M_{Torres}	M_{Direct}	0.220	(1.22, −0.12)
	M_{Henry}	M_{Direct}	0.184	(1.03, −0.05)
	M_{Padova}	M_{Direct}	0.181	(0.87, +0.30)

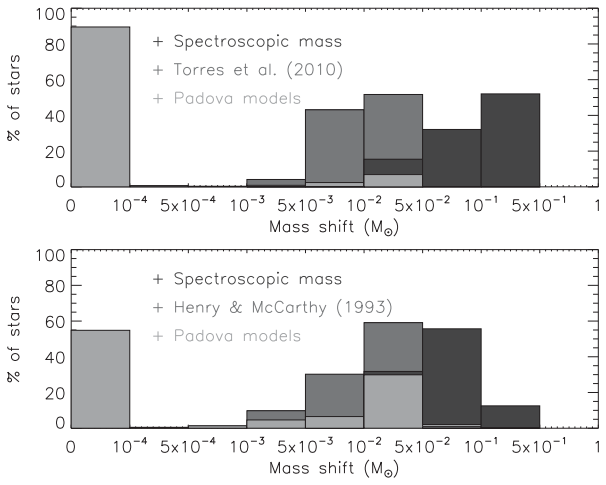

Figure 2. Impact of a 0.05 dex surface gravity (top) and 0.05 dex luminosity (bottom) increase on the mass predictions for data from Sousa et al. (2011a).

An initial inspection to our database showed no indication that the large uncertainties associated with some stars's global parameters could be responsible for the discrepancies found between the spectroscopic masses and the remaining predictions. For

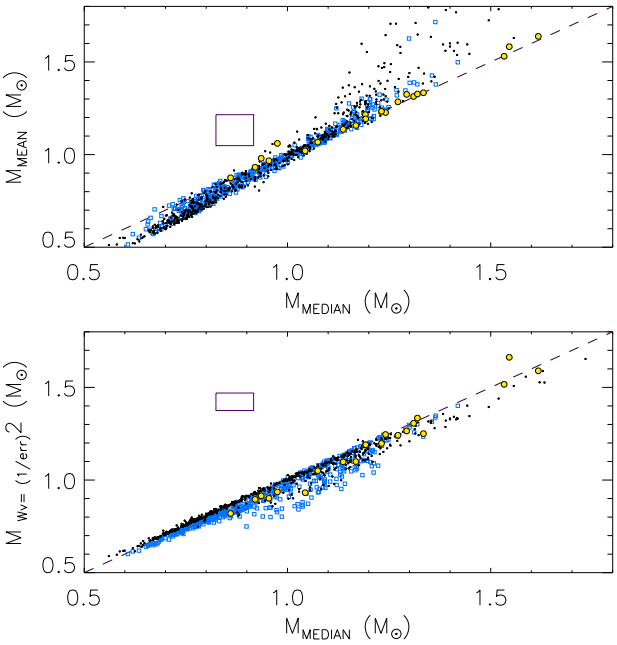

Figure 3. Comparison between the median of the four mass predictions and the mean (top) and the weighted mean (bottom) of the mass predictions. The squares and black dots correspond, respectively, to the Sousa et al. (2008, 2011b) data, while the circles correspond to the Bruntt et al. (2010) data. The boxes on the upper-left corners correspond to the typical mass uncertainties associated with each method, while the dashed lines correspond to the 1:1 relation.

Table 2. The rms of the four mass estimates (M_i) using three options for combining the values (mean, median and weighted average).

Data		Mean	Median	Weighted
Sousa et al. (2008)	$M_{\rm Spec}$	0.181	0.225	0.235
	$M_{\rm Torres}$	0.080	0.044	0.036
	$M_{\rm Henry}$	0.083	0.060	0.070
	$M_{\rm Padova}$	0.073	0.062	0.047
Sousa et al. (2011b)	$M_{\rm Spec}$	0.384	0.493	0.512
	$M_{\rm Torres}$	0.161	0.064	0.048
	$M_{\rm Henry}$	0.121	0.056	0.077
	$M_{\rm Padova}$	0.131	0.060	0.043

instance, in the lower-right panel of Fig. 4, we can notice that objects which display large discrepancies between the spectroscopic and median mass (i.e. that of the median of the four mass estimates) do not necessarily have large uncertainties on their surface gravity estimates. Indeed, even if we do not take into account the data points for which there are such large uncertainties (for instance luminosity or surface gravity uncertainty above 0.1 dex), which is the case for some of the largest mass/furthest stars, we still find a 2:1 relation between the median of the mass estimates and the spectroscopic masses (as seen in the upper-right panel of Fig. 4).

Likewise, we find no hints of a correlation between the targets' surface gravity or metal abundance and the differences between the mass estimates (cf. the lower-left panel of Fig. 4).

Nevertheless, we found hints of a correlation between the stars' effective temperature and luminosity and the mass discrepancies (as seen in the upper-left panel of Fig. 4). This should come as no surprise if we recall the well-known correlations between the mass, effective temperature and luminosity of main-sequence stars (Kippenhahn & Weigert 1990), and the fact that a linear fit to the spectroscopic masses and median of the mass estimates of all of Sousa et al.'s targets yields a function of the type $M_{\rm Spec} = 2.58 M_{\rm Median} - 1.53$.

On the other hand, the fact that the Bruntt et al. (2010) data do not show a significant discrepancy in the mass estimate obtained through any method, and given that in this case surface gravities were not obtained though spectroscopy, rises the suspicion that the problem may lie within the spectroscopic surface gravities.

These discrepancies between the asteroseismic and spectroscopic surface gravities are further corroborated by recent studies such as the one of Bruntt et al. (2012). In this particular case, we see that the differences between the spectroscopic surface gravities and the asteroseismic ones can be larger than the sum of the uncertainties associated with these parameters. Moreover, in fig. 1 of Bruntt et al. (2012), there are hints of a correlation between their targets' effective temperature and the discrepancy between the spectroscopic and asteroseismic surface gravities. Furthermore, in their work Bruntt et al. propose a calibration of their microturbulence values, which have a deep impact on the inference of spectroscopic surface gravities.

Comparing the targets' spectroscopic mass and microturbulence shown in Fig. 5, a relation between these two parameters is noticeable. This is expectable since both are correlated with the star's effective temperature. This suggests once more that a problem with microturbulence might have an impact on the spectroscopic surface gravity.

A microturbulence re-calibration for the Sousa et al. (2008, 2011b) data goes far beyond the objectives of this work. Nevertheless, we can proceed to an empirical calibration of the spectroscopic masses given the median of the four mass estimates. The upper panel of Fig. 6 shows the expected median of the mass estimates given an object's spectroscopic mass ($M_{\rm Spec}$). The dashed line corresponds to a quadratic fit to the data:

$$M_{\rm Median} = -0.097 M_{\rm Spec}^2 + 0.585 M_{\rm Spec} + 0.520. \quad (5)$$

A more ambitious step consists in determining what should be the re-calibration of the surface gravity. From an observational point of view, it is useful to compute this calibration as a function of the targets' effective temperature. In order to achieve this, we took into account the median of the four mass estimates and the physical relations used in the direct method. The lower panel of Fig. 6 shows a comparison between the effective temperatures of Sousa et al.'s targets against the difference between the spectroscopic surface gravities and those expected from the median of the four mass estimates. The dashed line corresponds to a cubic fit to the data, which can be seen as a possible method for re-calibrating the spectroscopic surface gravities:

$$\log(g_{\rm Median}) - \log(g_{\rm Spec}) = -290.03 \log(T_{\rm eff}/5777)^3 - 19.68 \log(T_{\rm eff}/5777)^2 - 3.16 \log(T_{\rm eff}/5777) - 0.02. \quad (6)$$

This function can be seen as an empirical calibration to the spectroscopic surface gravities if the object's effective temperature is known.

4 CONCLUSIONS AND FUTURE WORK

In this study, we have estimated the masses for about a thousand F-, G- and K-type stars using four different methods. These approaches include two empirical relationships, a comparison of

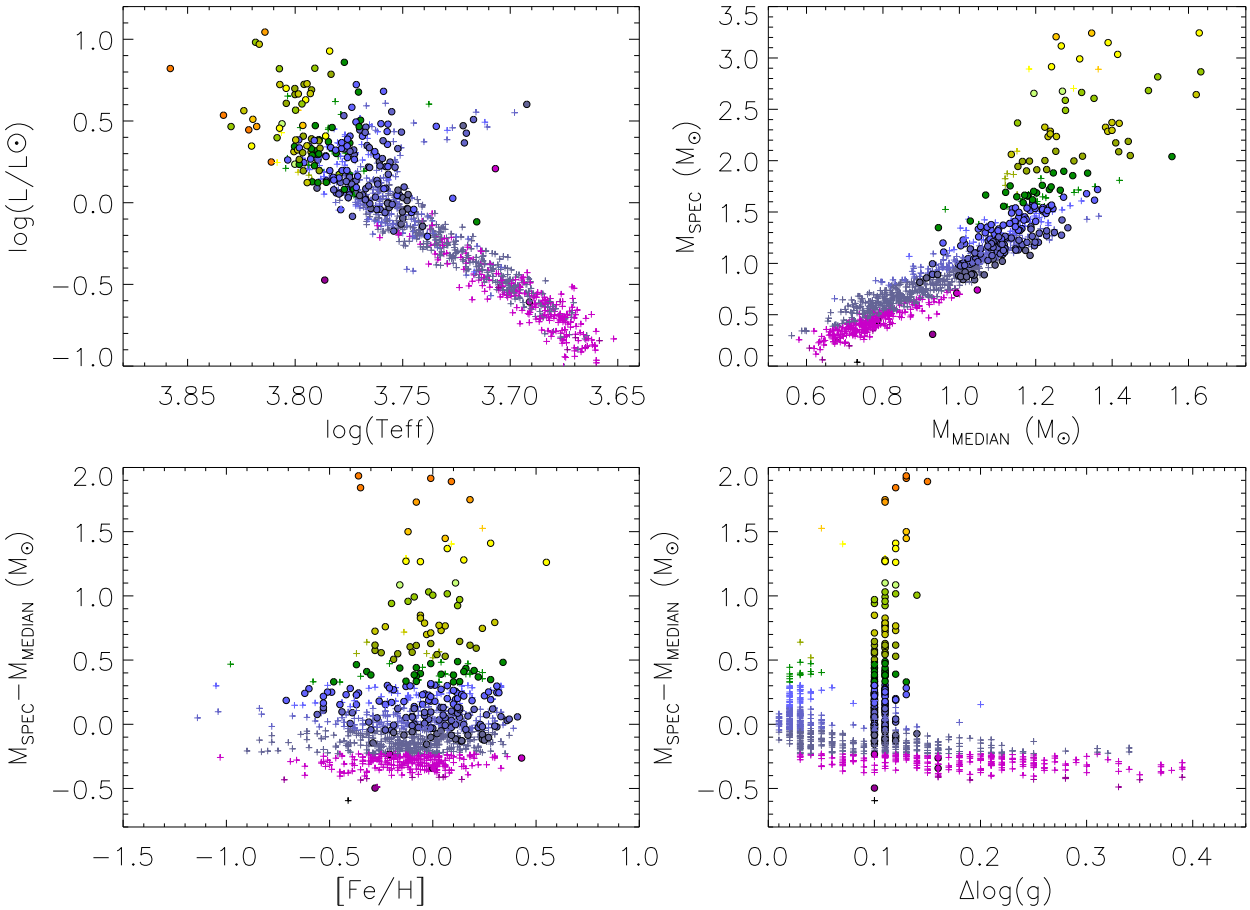

Figure 4. Top left: position of Sousa et al.'s stars in the HR diagram. Top right: comparison between the spectroscopic mass and the median of the four mass estimates. Bottom left: comparison of the metal abundance against the discrepancy between spectroscopic and the median mass discrepancy. Bottom right: same as the previous panel with respect to the surface gravity's uncertainties. The circles correspond to the targets with a high luminosity uncertainty, $\Delta\log(L/L_{\odot}) > 0.1$. The colour of each data point provides an indication of the discrepancy between its spectroscopic mass and the median of the four mass estimates (as seen in the lower panels).

global stellar parameters against theoretical models and a method which 'directly' takes into account the surface gravity and the luminosity–radius–effective temperature relation. In the latter case, spectroscopic surface gravities give rise to a spectroscopic mass estimation. A comparison between the different mass estimates shows that these methods produce fairly consistent results, except in the case of the computation of the spectroscopic masses. The result is also consistent for the Sousa et al. (2008, 2011b) data. An extension of this analysis to the Bruntt et al. (2010) data seems to indicate that, as in the case of the work of Bruntt et al. (2012), the problem should lie within the spectroscopic surface gravities used in this work.

Concerning the combination of the mass estimates, our results indicate that the use of a weighted average and the median produces similar results. Indeed, our analysis does not show any particular advantage in the use of a weighed mean with respect to the median.

For the four methods evaluated here, Torres et al.'s empirical approach is the one that gives the best agreement (i.e. the smallest rms) with respect to the weighted mean of the four mass estimates. On the other hand, regarding the median, the best agreement occurs for Henry & McCarthy's MLR (although Torres et al.'s method presents similar agreement).

Finally, our final mass estimate allows us to derive an expression for 'predicting' what should be the median of the four mass estimates given a set of spectroscopic masses. Of greater relevance is the expression obtained for an empirical 'correction' to the spectroscopic surface gravities derived using the Sousa et al. (2008) approach. It is of utmost importance to determine if this method (or a similar one) can be applied to spectroscopic surface gravities derived using other procedures.

In the present work, we have discussed the use of a weighted mean in which the weights are proportional to the uncertainties associated with each mass estimate (i.e. $w_i = 1/\sigma_i^2$). In addition, one can associate with each weight a quality factor Q_i, which reflects each method's reliability, corresponding to a weight $w_i = Q_i/\sigma_i^2$). In order to calibrate these quality factors, we would require a data sample for which stellar masses have been derived through an independent method (such as the use of binary stars or asteroseismology). Nevertheless, as shown here, the reliability of a given method clearly depends on the reliability of global stellar parameters required by each method and, thus, on the way how each parameter has been derived. Therefore, the calibration of the quality factors for a specific sample might not be valid for a different sample.

Concerning the spectroscopic surface gravities, Creevey & Thévenin (2012) and Creevey et al. (2013) present an alternative to the use of asteroseismic surface gravities. Moreover, in the case of planetary transits, one can use photometric light curves in order to derive accurate surface gravities (Torres et al. 2012; Mortier et al.

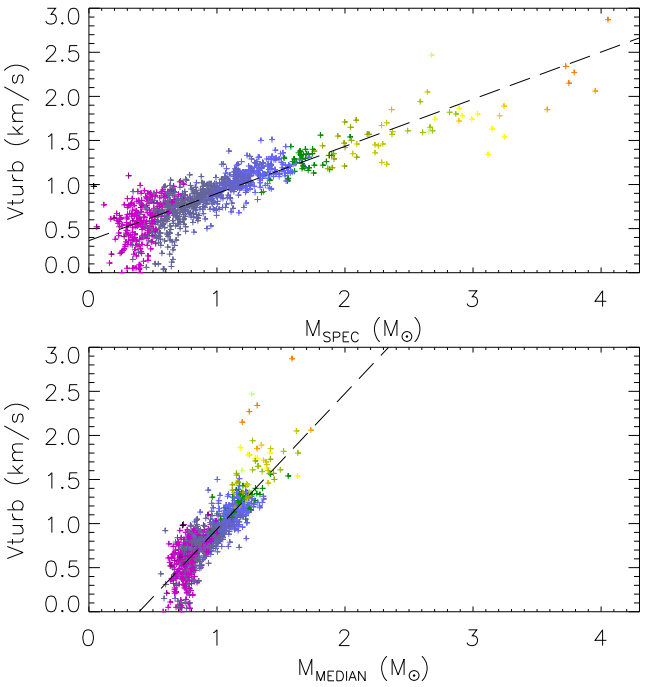

Figure 5. Comparison between the microturbulent velocity against the spectroscopic mass (top) and the median of the four mass estimates (bottom) for Sousa et al.'s data. Each data point's colour provides an indication of the discrepancy between its spectroscopic mass and the median of the four mass estimates (as seen in Fig. 4). The dashed lines correspond to the best linear fits to the data, respectively: $V_{\rm turb} = 0.53M_{\rm Spec} + 0.36$ and $V_{\rm turb} = 1.54M_{\rm Median} - 0.60$.

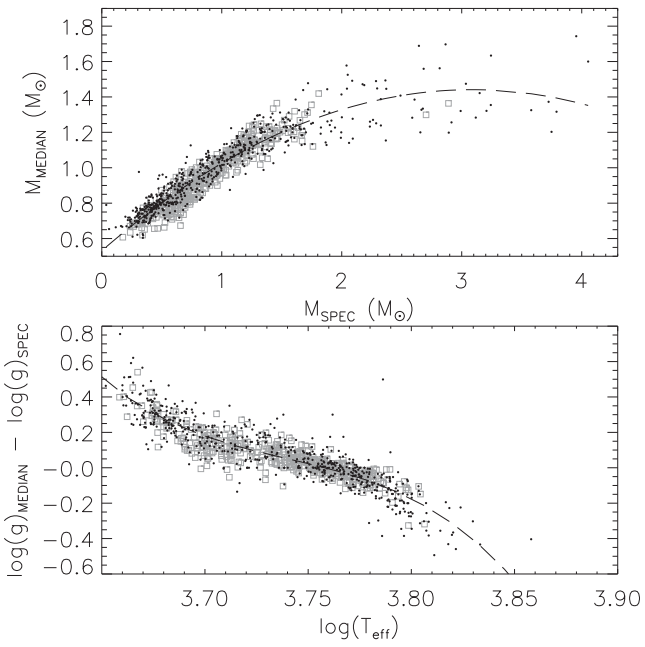

Figure 6. Top: empirical calibration of the stellar mass given the spectroscopic masses. Bottom: calibration of the surface gravities given an object's effective temperature. The squares and black dots correspond, respectively, to the Sousa et al. (2008, 2011b) data. The black lines correspond to two polynomialfits to the data.

2013b). Such possibilities will be taken into account in a future investigation of the systematic difference between the spectroscopic surface gravity estimations and the predictions resulting from other approaches. Moreover, we will also address the important issue of the calibration of the spectroscopic predictions.

ACKNOWLEDGEMENTS

We thank the anonymous referee for the valuable remarks. Support was provided by FCT under project /PTDC/CTE-AST/66181/2006 and the /SFRH/BPD/37491/2007 research grant of FJGP, both co-financed by the European Social Fund. MSC is supported by an Investigador FCT contract funded by FCT/MCTES (Portugal) and POPH/FSE (EC) and by funds from the ERC, under FP7/EC, through the project FP7-SPACE-2012-31284. NCS, SGS, and AM acknowledge the support by the European Research Council/European Community under the FP7 through Starting Grant agreement number 239953. NCS is supported by FCT through the Investigador FCT contract reference IF/00169/2012 and POPH/FSE (EC) by FEDER funding through the programme 'Programa Operacional de Factores de Competitividade – COMPETE'. We have used the CDS-Strasbourg Database.

REFERENCES

Andersen J., 1991, A&AR, 3, 91
Bigot L. et al., 2011, A&A, 534, L3
Brown T. M., Gilliland R. L., Noyes R. W., Ramsey L. W., 1991, ApJ, 368, 599
Bruntt H. et al., 2010, MNRAS, 405, 1907
Bruntt H. et al., 2012, MNRAS, 423, 122
Chaplin W. J. et al., 2014, ApJS, 210, 1
Creevey O. L., Thévenin F., 2012, in Boissier S., de Laverny P., Nardetto N., Samadi R., Valls-Gabaud D., Wozniak H., eds, SF2A-2012: Proc. Annual Meeting of the French Society of Astronomy and Astrophysics, Asteroseismic Constraints for Gaia. p. 189
Creevey O. L. et al., 2013, MNRAS, 431, 2419
Fernandes J., Santos N., 2004, A&A, 427, 607
Fernandes J., Vaz A., Vicente L., 2011, A&A, 532, A20
Flower P. J., 1996, ApJ, 469, 355
Gafeira R., Patacas C., Fernandes J., 2012, Ap&SS, 341, 405
Henry T., 2004, in Hilditch R. W., Hensberge H., Pavlovski K., eds, ASP Conf. Ser. Vol. 318, Spectroscopically and Spatially Resolving the Components of the Close Binary Stars. Astron. Soc. Pac., San Francisco, p. 159
Henry T., McCarthy D. J., 1993, AJ, 106, 773
Huber D. et al., 2012, ApJ, 760, 32
Johnson J. A., Aller K. M., Howard A. W., Crepp J. R., 2010, PASP, 122, 905
Kippenhahn R., Weigert A., 1990, Stellar Structure and Evolution. Springer-Verlag, Berlin
Kjeldsen H., Bedding T. R., 1995, A&A, 293, 87
Kjeldsen H., Bedding T. R., Christensen-Dalsgaard J., 2009, in Pont F., Sasselov D., Holman M. J., eds, Proc. IAU Symp. 253, Transiting Planets. Cambridge Univ. Press, Cambridge, p. 309
Lo Curto G. et al., 2010, A&A, 512, A48
Mathur S. et al., 2012, ApJ, 749, 152
Mayor M. et al., 2003, The Messenger, 114, 20
Metcalfe T. et al., 2010, ApJ, 723, 1583
Mortier A., Santos N., Sousa S., Israelian G., Mayor M., Udry S., 2013a, A&A, 551, A112
Mortier A., Santos N. C., Sousa S. G., Fernandes J. M., Adibekyan V. Z., Delgado Mena E., Montalto M., Israelian G., 2013b, A&A, 558, A106
Neves V., Bonfils X., Santos N. C., Delfosse X., Forveille T., Allard F., Udry S., 2013, A&A, 551, A36

Santos N. C., Israelian G., Mayor M., 2004, A&A, 415, 1153
Santos N. C., Israelian G., Mayor M., Bento J. P., Almeida P. C., Sousa S. G., Ecuvillon A., 2005, A&A, 437, 1127
Santos N. C. et al., 2013, A&A, 556, A150
Sousa S. G., Santos N. C., Israelian G., Mayor M., Monteiro M. J. P. F. G., 2006, A&A, 458, 873
Sousa S. G. et al., 2008, A&A, 487, 373
Sousa S. G., Santos N. C., Israelian G., Lovis C., Mayor M., Silva P. B., Udry S., 2011a, A&A, 526, A99
Sousa S. G., Santos N. C., Israelian G., Mayor M., Udry S., 2011b, A&A, 533, A141
Torres G., 2010, AJ, 140, 1158
Torres G., Andersen J., Giménez A., 2010, A&AR, 18, 67
Torres G., Fischer D. A., Sozzetti A., Buchhave L. A., Winn J. N., Holman M. J., Carter J. A., 2012, ApJ, 757, 161
Ulrich R. K., 1986, ApJ, 306, L37
van Leeuwen F., 2007, A&A, 474, 653
Xia F., Fu Y.-N., 2010, Chin. Astron. Astrophys., 34, 277

APPENDIX A: MASS ESTIMATES ACCORDING TO THE DIFFERENT METHODS

The following tables contain the mass estimates obtained according to the four methods presented here (plus the median of these four mass estimates) for the Sousa et al. (2008, 2011b) targets and those of Bruntt et al. (2010).

Table A1. Mass estimate for the Sousa et al. (2008) targets according to different methods (in solar units).

Star ID	$M_{\rm Direct}$		$M_{\rm Torres}$		$M_{\rm Henry}$		$M_{\rm Padova}$		$M_{\rm Median}$		Star ID	$M_{\rm Direct}$		$M_{\rm Torres}$		$M_{\rm Henry}$		$M_{\rm Padova}$		$M_{\rm Median}$	
	M	ΔM	M	ΔM	M	ΔM	M	ΔM	M	ΔM		M	ΔM	M	ΔM	M	ΔM	M	ΔM	M	ΔM
HD 55	0.639	0.046	0.340	0.349	0.704	0.055	0.600	0.054	0.619	0.038	HD 16714	0.940	0.060	0.777	0.119	0.982	0.074	0.833	0.051	0.886	0.059
HD 142	1.205	0.079	2.703	0.779	1.298	0.097	1.300	0.052	1.299	0.047	HD 17051	1.202	0.077	1.486	0.372	1.177	0.088	1.200	0.051	1.201	0.049
HD 283	0.768	0.050	0.632	0.182	0.858	0.066	0.716	0.053	0.742	0.048	HD 17970	0.777	0.053	0.616	0.231	0.873	0.066	0.731	0.052	0.754	0.052
HD 361	1.026	0.065	1.264	0.118	1.057	0.079	1.046	0.051	1.051	0.043	HD 18386	1.008	0.066	0.618	0.160	0.944	0.072	0.950	0.056	0.947	0.045
HD 750	0.812	0.054	0.492	0.188	0.845	0.065	0.743	0.053	0.777	0.034	HD 18719	0.896	0.059	0.633	0.204	0.904	0.069	0.814	0.054	0.855	0.038
HD 870	0.926	0.060	0.620	0.136	0.921	0.069	0.852	0.054	0.887	0.039	HD 19034	0.875	0.056	0.734	0.123	0.971	0.073	0.762	0.051	0.819	0.048
HD 967	0.835	0.053	0.964	0.167	0.989	0.075	0.738	0.051	0.899	0.060	HD 19467	1.037	0.066	1.057	0.054	1.124	0.084	0.911	0.051	1.047	0.040
HD 1237	0.983	0.064	0.877	0.265	0.966	0.072	0.957	0.054	0.962	0.043	HD 19994	1.246	0.081	2.890	0.558	1.382	0.103	1.346	0.064	1.364	0.062
HD 1320	0.951	0.060	0.901	0.096	1.002	0.075	0.866	0.054	0.926	0.046	HD 20003	0.990	0.064	0.828	0.188	0.991	0.074	0.900	0.054	0.945	0.052
HD 1388	1.103	0.070	1.152	0.099	1.133	0.085	1.070	0.052	1.118	0.040	HD 20407	0.957	0.061	1.060	0.045	1.060	0.079	0.904	0.052	1.008	0.034

Table A2. Mass estimate for the Sousa et al. (2011b) targets according to different methods (in solar units).

Star ID	$M_{\rm Direct}$		$M_{\rm Torres}$		$M_{\rm Henry}$		$M_{\rm Padova}$		$M_{\rm Median}$		Star ID	$M_{\rm Direct}$		$M_{\rm Torres}$		$M_{\rm Henry}$		$M_{\rm Padova}$		$M_{\rm Median}$	
	M	ΔM	M	ΔM	M	ΔM	M	ΔM	M	ΔM		M	ΔM	M	ΔM	M	ΔM	M	ΔM	M	ΔM
HD 67	1.024	0.065	0.883	0.297	0.983	0.074	1.000	0.054	0.991	0.038	HD 4597	1.023	0.065	1.153	0.388	1.137	0.086	0.939	0.053	1.080	0.077
HD 208	1.005	0.064	1.230	0.403	1.112	0.083	0.911	0.053	1.058	0.070	HD 4838	0.702	0.045	0.551	0.317	0.730	0.055	0.700	0.053	0.701	0.042
HD 457	1.230	0.078	1.881	0.598	1.262	0.095	1.220	0.051	1.246	0.047	HD 5349	1.179	0.083	0.741	0.396	1.126	0.085	0.968	0.052	1.047	0.048
HD 564	1.015	0.064	1.258	0.436	1.085	0.082	0.994	0.058	1.050	0.053	HD 5388	1.185	0.076	2.043	0.644	1.447	0.108	1.198	0.069	1.323	0.080
HD 1171	0.808	0.052	0.462	0.214	0.845	0.065	0.728	0.054	0.768	0.040	HD 6718	1.019	0.065	1.104	0.357	1.071	0.080	0.944	0.054	1.045	0.054
HD 1979	0.972	0.062	1.067	0.395	1.014	0.077	0.955	0.054	0.993	0.045	HD 8038	1.062	0.067	1.088	0.366	1.058	0.080	1.042	0.053	1.060	0.051
HD 2014	0.857	0.056	0.491	0.277	0.850	0.065	0.779	0.052	0.815	0.047	HD 8535	1.169	0.074	1.356	0.432	1.203	0.090	1.172	0.052	1.187	0.055
HD 2567	1.179	0.075	1.686	0.559	1.221	0.092	1.183	0.051	1.202	0.062	HD 8930	0.956	0.061	0.913	0.286	0.994	0.075	0.922	0.055	0.939	0.046
HD 2768	0.991	0.063	0.676	0.259	0.972	0.074	0.912	0.054	0.942	0.046	HD 8985	1.187	0.078	3.748	1.539	1.203	0.090	1.193	0.055	1.198	0.051
HD 3220	1.000	0.063	0.864	0.294	1.014	0.076	0.985	0.051	0.993	0.047	HD 9578	1.135	0.072	1.401	0.500	1.140	0.086	1.155	0.054	1.147	0.043

Table A3. Mass estimate for Bruntt et al. targets according to different methods (in solar units).

Star ID	$M_{\rm Direct}$		$M_{\rm Torres}$		$M_{\rm Henry}$		$M_{\rm Padova}$		$M_{\rm Median}$		Star ID	$M_{\rm Direct}$		$M_{\rm Torres}$		$M_{\rm Henry}$		$M_{\rm Padova}$		$M_{\rm Median}$	
	M	ΔM	M	ΔM	M	ΔM	M	ΔM	M	ΔM		M	ΔM	M	ΔM	M	ΔM	M	ΔM	M	ΔM
β Hyi	1.224	0.120	1.159	0.578	1.354	0.101	1.127	0.058	1.192	0.088	αCen B	0.925	0.072	1.027	0.548	0.916	0.069	0.859	0.059	0.920	0.055
τCet	0.799	0.059	1.002	0.526	0.921	0.069	0.776	0.052	0.860	0.062	HR5803	1.228	0.109	1.486	0.738	1.348	0.101	1.239	0.070	1.293	0.088
ιHor	1.185	0.098	1.212	0.595	1.175	0.088	1.200	0.062	1.192	0.062	γSer	1.166	0.105	1.296	0.631	1.324	0.099	1.148	0.070	1.231	0.085
αFor	1.214	0.120	1.522	0.780	1.455	0.109	1.145	0.084	1.334	0.114	μAra	1.160	0.100	1.248	0.648	1.177	0.088	1.045	0.058	1.168	0.074
δEri	1.144	0.130	1.225	0.624	1.282	0.096	1.257	0.073	1.241	0.083	70 Oph A	0.922	0.067	1.175	0.583	0.949	0.071	0.874	0.067	0.935	0.054
Procyon	1.463	0.140	1.566	0.777	1.594	0.119	1.500	0.077	1.533	0.093	ηSer	1.653	0.219	1.438	0.697	1.803	0.136	1.435	0.181	1.546	0.167
171 Pup	0.888	0.075	1.020	0.504	1.137	0.085	0.822	0.051	0.954	0.098	βAql	1.210	0.135	1.357	0.674	1.459	0.110	1.282	0.120	1.320	0.126
ξHya	2.125	0.269	2.811	1.372	2.404	0.180	2.848	0.088	2.607	0.233	δPav	1.120	0.095	1.057	0.516	1.092	0.082	1.000	0.060	1.074	0.068
βVir	1.284	0.112	1.326	0.644	1.351	0.101	1.295	0.067	1.310	0.071	γPav	0.948	0.074	1.140	0.580	1.159	0.087	0.836	0.054	1.043	0.100
ηBoo	1.489	0.159	1.830	1.045	1.644	0.123	1.590	0.068	1.617	0.095	τPsA	1.238	0.106	1.378	0.693	1.306	0.098	1.218	0.059	1.272	0.077
αCen A	1.128	0.092	1.209	0.623	1.146	0.086	1.062	0.060	1.137	0.065	νInd	0.960	0.112	0.990	0.487	1.477	0.111	0.815	0.052	0.975	0.171

SUPPORTING INFORMATION

Additional Supporting Information may be found in the online version of this article:

Mass estimate for the Sousa et al. (2008) targets according to different methods.
Mass estimate for the Sousa et al. (2011b) targets according to different methods.
Mass estimate for the Bruntt et al. (2010) targets according to different methods (http://mnras.oxfordjournals.org/lookup/suppl/doi:10.1093/mnras/stu1812/-/DC1).

Please note: Oxford University Press are not responsible for the content or functionality of any supporting materials supplied by the authors. Any queries (other than missing material) should be directed to the corresponding author for the article.

This paper has been typeset from a TEX/LATEX file prepared by the author.